Journal Pre-proofs

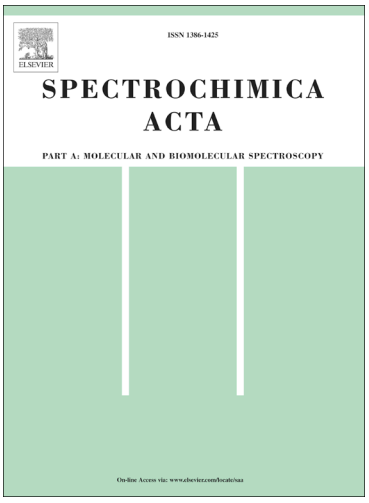

Rapid and selective visualization of mitochondrial hypochlorite by a red region water-soluble fluorescence probe

Tian-Ran Wang, Xiao-Fan Zhang, Xiao-Qing Huang, Xiao-Qun Cao, Shi-Li Shen

PII: S1386-1425(20)31094-5
DOI: https://doi.org/10.1016/j.saa.2020.119115
Reference: SAA 119115

To appear in: *Spectrochimica Acta Part A: Molecular and Biomolecular Spectroscopy*

Received Date: 18 July 2020
Revised Date: 4 October 2020
Accepted Date: 16 October 2020

Please cite this article as: T-R. Wang, X-F. Zhang, X-Q. Huang, X-Q. Cao, S-L. Shen, Rapid and selective visualization of mitochondrial hypochlorite by a red region water-soluble fluorescence probe, *Spectrochimica Acta Part A: Molecular and Biomolecular Spectroscopy* (2020), doi: https://doi.org/10.1016/j.saa.2020.119115

This is a PDF file of an article that has undergone enhancements after acceptance, such as the addition of a cover page and metadata, and formatting for readability, but it is not yet the definitive version of record. This version will undergo additional copyediting, typesetting and review before it is published in its final form, but we are providing this version to give early visibility of the article. Please note that, during the production process, errors may be discovered which could affect the content, and all legal disclaimers that apply to the journal pertain.

© 2020 Elsevier B.V. All rights reserved.

Rapid and selective visualization of mitochondrial hypochlorite by a red region water-soluble fluorescence probe

Tian-Ran Wang[ac,1], Xiao-Fan Zhang[b,1], Xiao-Qing Huang[ac,1], Xiao-Qun Cao[ac], Shi-Li Shen[ac,*]

[a] *School of Chemistry and Pharmaceutical Engineering, Shandong First Medical University & Shandong Academy of Medical Sciences, Taian, Shandong 271016, P. R. China*

[b] *Taian Center For Food and Drug Control, Taian 271000, P. R. China*

[c] *Institute of optical functional materials for biomedical imaging, School of Chemistry and Pharmaceutical Engineering, Shandong First Medical University & Shandong Academy of Medical Sciences, Taian, Shandong 271016, P. R. China*

Corresponding Author: Dr. Shi-Li Shen

E-mail address: slshen86@163.com (S.L. Shen)

Tel.: +86-538-6229741; Fax: +86-538-6229741

[1] These authors have equal contribution.

Journal Pre-proofs

Abstract

Hypochlorite ($^{-}$OCl) has long been recognized as an effective microbicidal agent in immune system. Herein, we report the design, preparation and spectral characteristics of a $^{-}$OCl fluorescent probe (**FI-Mito**). The probe exhibited remarkable fluorescence turn-on signal in the red region upon $^{-}$OCl titration with the detection limit as low as 0.9 nM. **FI-Mito** displayed specific response for $^{-}$OCl in completely aqueous solution. Meanwhile, the introduction of quaternized pyridine realized mitochondria-targeting ability. **FI-Mito** was further applied to monitor the generation of endogenous $^{-}$OCl in the mitochondria of macrophage cells and mice. Therefore, it was established that **FI-Mito** may serve as a useful molecular tool for $^{-}$OCl detection in vivo.

Keywords:

Fluorescent probe; Hypochlorite; Mitochondrion; In vivo; Water-soluble; Red region

1. Introduction

Hypochlorous acid (HOCl), a kind of important reactive oxygen species (ROS), is generated from H_2O_2 and Cl^- catalyzed by enzyme myeloperoxidase (MPO) in phagosomes [1,2]. At physiological pH, a part of HOCl could dissociate to hypochlorite ($^{-}$OCl), which is a household bleaching agent and disinfectant of drinking water [3]. On the other hand, $^{-}$OCl governs numerous critical biological processes. Despite this, the excessive production of $^{-}$OCl may have detrimental effects on host tissues, thus leading to many disorders such as cardiovascular diseases, neurodegeneration and cancer [4-6]. In this regard, it is worth searching for appropriate tools to detect the real-time level of $^{-}$OCl quantitatively.

Fluorescence probe has attracted significant interest in the field of $^{-}$OCl detection due to its high sensitivity and selectivity, unparalleled resolution, easy operation and capability of real-time sensing. Nowadays, many selective fluorescent probes for $^{-}$OCl

have been reported [7-14]. However, the emission peak was mainly located in ultraviolet or visible region (300-650 nm), which may inevitably restrict the application in living systems. To our delight, fluorescent probes emitting in the far-red to near-infrared range (600-900 nm) showed deep tissue penetration ability and weak auto fluorescence interference [15-17].

Much evidence indicated that mitochondrion was the main source of ROS [18]. So great efforts have been made towards the development of $^{-}$OCl sensors especially applied in mitochondria. Particularly, the probe with accurate mitochondria-targeting ability could act as a useful tool to elucidate the subcellular distribution of $^{-}$OCl [19-21]. Yet, $^{-}$OCl probes with far-red to near-infrared emission that could target mitochondria are still in great demand [22].

Enlightened by the above considerations, we developed a turn-on fluorescent probe (**FI-Mito**) for the specific detection of $^{-}$OCl. Compared with the prior probes reported in the literature, **FI-Mito** showed distinctive advantages: first, the probe possessed longer emission (in the range of 600-700 nm), which was in the far-red to near-infrared range [23,24]; secondly, the addition of $^{-}$OCl to the solution of **FI-Mito** led to greatly enhanced fluorescence (about 27-fold increase), demonstrating its high sensitivity (detection limit: 0.9 nM) [25]; last but not least, **FI-Mito** was water-soluble (no organic solvent was used in the test conditions), superior to other probes which needed a content of organic solvent for sample analysis in vitro [26,27]. Also, the presence of the quaternized pyridine group enabled its mitochondria-targeting ability [28]. In addition, **FI-Mito** was successfully applied in fluorescence imaging of endogenously produced $^{-}$OCl in living cells as well as in mice.

2. Experimental

2.1 Materials and instrumentation

NMR spectra were collected on a Bruker Avance spectrometer, using d_6-DMSO as a solvent and resonances (δ) were given in ppm relative to tetramethylsilane (TMS). Coupling constants (J values) were reported in hertz. UV-Vis and

fluorescence spectra were obtained on the Hitachi U-4100 spectrophotometer and Perkin-Elmer LS-55 luminescence spectrophotometer, respectively. High-resolution mass spectroscopy (HR-MS) was performed on the Q-TOF6510 spectrograph (Agilent).

ROS and reactive nitrogen species (RNS) solution was prepared according to the previous report [29]. Unless otherwise noted, chemical reagents were purchased from merchants and used without further purification. Ultrapure water (over 18 MΩ·cm) was produced from a Milli-Q reference system (Millipore) and then used throughout all experiments.

2.2 UV-Vis and fluorescence spectroscopy studies

For the preparation of tested samples, probe **FI-Mito** was dissolved in PBS to afford the tested samples. Then the tested mixture was transferred to a quartz cuvette with 1-cm path length to measure absorbance against the corresponding reagent blank or fluorescence spectra with excitation wavelength of 580 nm.

*2.3 Synthesis of probe **FI-Mito***

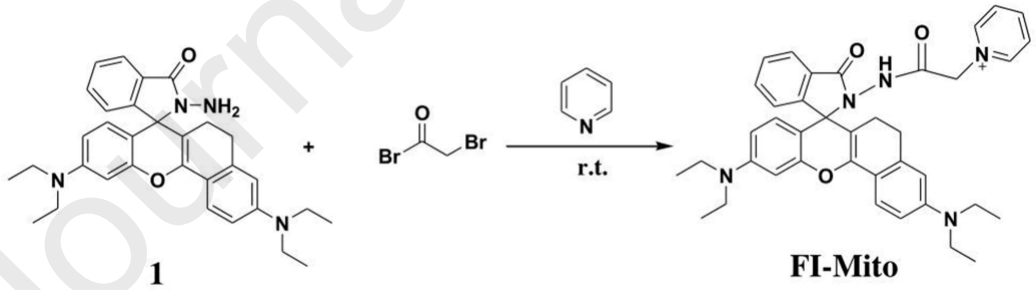

Scheme 1 Synthesis route of probe **FI-Mito**.

The synthetic route of **FI-Mito** was shown in Scheme 1, in which compounds **1** was prepared by the literatures [30,31]. The solution of compound **1** (0.8 mmol) in 6 mL dry pyridine was stirred for 30 min at room temperature and then bromoacetyl bromide (0.96 mmol) was added. The mixture was stirred for 12 h under N_2

atmosphere. And then the mixture was poured into 100 mL ethyl acetate and 100 mL saline. The organic layer was washed for three times with saline water (100 mL), dried over anhydrous Na_2SO_4 and filtered. The solvent was concentrated under reduced pressure, and the residue was purified by column chromatography on silica gel using dichloromethane/methanol (80/1, v/v) as eluent to afford a green solid **FI-Mito** in 24.7% yield. ^{1}H NMR (400 MHz, DMSO-d_6), δ (ppm): 10.53 (s, 1H), 8.81 (d, J = 5.7 Hz, 2H), 8.58 (t, J = 7.7 Hz, 1H), 8.07 (t, J = 6.7 Hz, 2H), 7.79 (d, J = 7.1 Hz, 1H), 7.61-7.51 (m, 3H), 7.16 (d, J = 7.5 Hz, 1H), 6.73-6.48 (m, 1H), 6.43 (s, 2H), 6.33 (d, J = 8.8 Hz, 2H), 5.47 (s, 2H), 3.36 (d, J = 6.5 Hz, 8H), 2.48-2.36 (m, 2H), 2.13-1.70 (m, 1H), 1.56-1.47 (m, 1H), 1.10 (t, J = 6.0 Hz, 12H). ^{13}C NMR (100 MHz, DMSO-d_6), δ (ppm): 165.09, 163.45, 153.18, 149.67, 148.59, 148.09, 147.31, 146.54, 146.14, 138.57, 133.46, 129.12, 128.01, 124.03, 123.49, 122.99, 116.91, 110.77, 109.01, 108.69, 99.39, 97.67, 67.07, 61.21, 44.10, 28.47, 21.73, 12.97. HRMS m/z: calcd for $C_{39}H_{42}N_5O_3^+$ $[M]^+$: 628.3288; found: 628.3294.

2.4 Cell culture and imaging

RAW264.7 cells (Cell Bank of the Chinese Academy of Sciences, China) were cultured in DMEM supplemented with 10% FBS in the humidified atmosphere of 95% air and 5% CO_2 at 37 ℃.

For the fluorescence imaging of endogenous $^-$OCl with **FI-Mito**, RAW264.7 cells were incubated with lipopolysaccharide (LPS, 1 μg/mL) for 6 h, and further incubated with phorbol 12-myristate 13-acetate (PMA, 1 μg/mL) for 30 min, and then 1 μM **FI-Mito** for 30 min. The cells were washed with PBS (pH 7.4) for three times, and then fluorescence imaging of cells was performed on a Leica SP8 confocal laser scanning microscope with excitation at 561 nm through a 20 × 0.7 NA objective; the corresponding fluorescence emissions were collected at 645-700 nm.

2.5 In vivo imaging of $^-$OCl in the mouse model

All animal procedures were performed in accordance with the guidelines of the Institutional Animal Care and Use Committee. 6-8 week-old female Kunming mouse

was selected as the mouse model. In the mouse model experiment, **FI-Mito** was first dissolved in DMSO to afford the stock solution (5 mM). Then the concentration of **FI-Mito** was diluted to 50 μM by adding 990 μL of saline into 10 μL of stock solution. The experimental leg (right) and control leg (left) was given an injection of LPS (5 μg/mL, 50 μL) and saline (50 μL), respectively. After 12 h, 50 μL of **FI-Mito** (50 μM in saline, containing 1% DMSO) was injected into the same area in both of the legs. Then the mice were anesthetized and imaged by the in-vivo imaging system (In-Vivo Master, Wuhan Grandimaging Technology Co., LTD). 635 nm continuous wavelength laser was employed as the light source, and the signal was collected using a 676±30 nm bandpass filter.

3. Results and discussion

*3.1 Design and synthesis of **FI-Mito***

Rhodamine is a desirable platform in the design of fluorescence probes because of its preeminent photophysical properties, including high quantum yield and high molar extinction coefficient [32]. Moreover, the introduction of quaternized pyridine group has provided a useful tool for the mitochondrial $^{-}$OCl detection. Target probe **FI-Mito** was synthesized facilely (Scheme 1) and fully characterized by ^{1}H NMR, ^{13}C NMR and HRMS (Fig. S1-S3, ESI†).

*3.2 Spectroscopic response of **FI-Mito** to $^{-}$OCl*

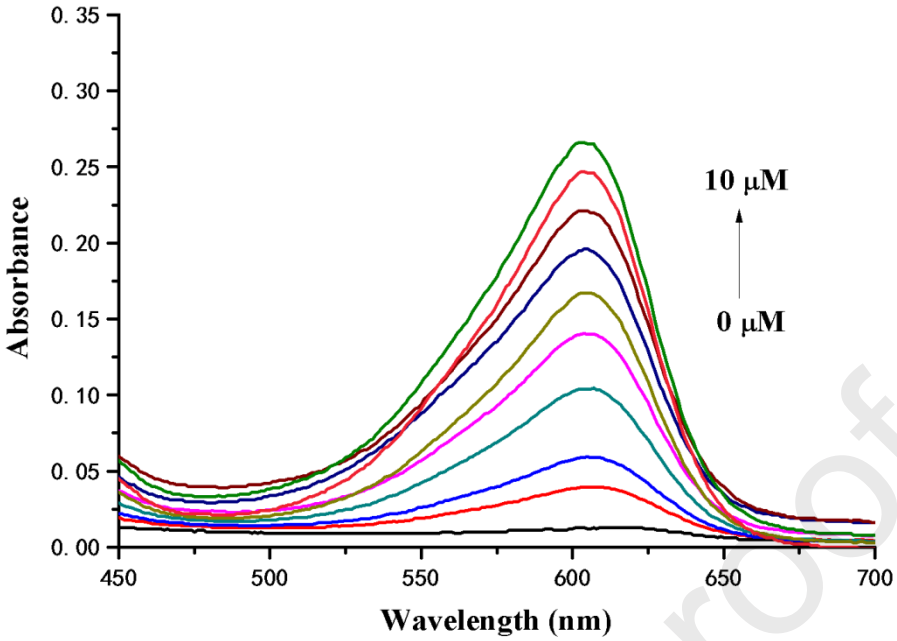

Figure 1 Absorption spectral changes of **FI-Mito** (10 μM) along with the titration of $^{-}$OCl in PBS buffer solution (pH = 8).

It was worth noting that the probe's excellent water solubility avoided the co-existence of organic solvent, which was crucial for $^{-}$OCl detection in biological specimens. Because organic solvent may destroy the normal function of biomolecules. The absorption and emission spectra of probe **FI-Mito** were investigated in 100% aqueous solution. As displayed in Fig. 1, absorption spectra of **FI-Mito** with increasing dose of $^{-}$OCl indicated a gradual increase of the absorption peak at 603 nm. The changes should be due to the interaction of **FI-Mito** and $^{-}$OCl. Rhodamine group existed in the ring-closed spirolactam structure in the absence of $^{-}$OCl. However, the addition of $^{-}$OCl led to the ring-opening of rhodamine. Many literature reports about $^{-}$OCl fluorescent probes were based on the proposed mechanism outlined in Scheme 2 [33-35].

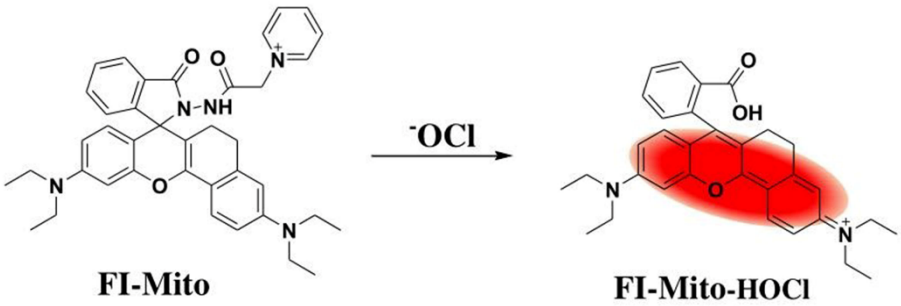

Scheme 2 Sensing mechanism of **FI-Mito** to $^{-}$OCl.

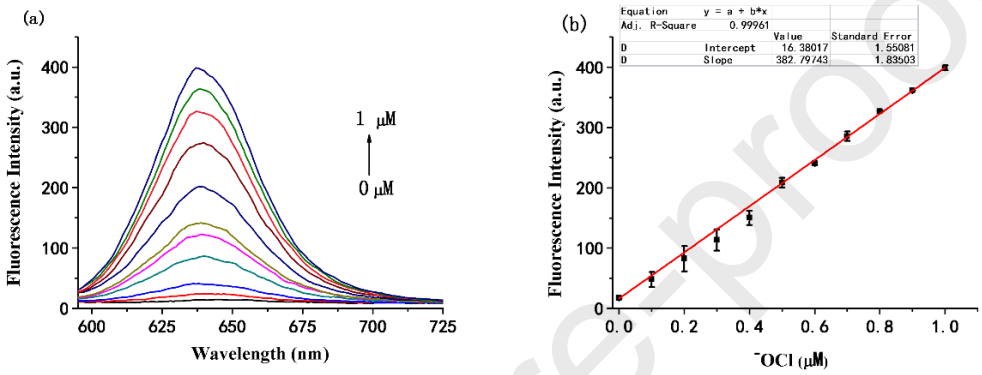

Figure 2 (a) Fluorescence emission spectra and (b) fluorescence intensity (I_{637}) of **FI-Mito** (1 μM) along with the addition of $^{-}$OCl in PBS buffer solution (pH = 8). The fluorescent spectra were obtained with λex = 580 nm.

Next, the fluorescent titration spectra of **FI-Mito** toward $^{-}$OCl were investigated (Fig. 2). As expected, the free probe almost exhibited no fluorescence in the emission window of 600-700 nm. Upon treatment with $^{-}$OCl, probe **FI-Mito** displayed the featured emission peak of rhodamine locating at 637 nm (Fig. 2a). Furthermore, we analyzed the dependence of fluorescence intensity (I_{637}) on the dose of $^{-}$OCl. As shown in Fig. 2b, I_{637} had a dramatic increase from 14 to 399, up to 27-fold enhancement. A linear relationship existed between I_{637} signal and $^{-}$OCl concentration from 0 to 1 μM. Also, the detection limit was determined to be 0.9 nM. The data established that **FI-Mito** possessed outstanding sensitivity toward $^{-}$OCl, which was potential for fluorescence imaging in certain biological environments.

In order to verify the sensing mechanism of **FI-Mito** for $^{-}$OCl, the mixture solution of **FI-Mito** and $^{-}$OCl was analyzed by HRMS (Fig. S4, ESI†). Fig. S4

showed a peak at m/z = 495.2634, which was assigned to the product **FI-Mito-HOCl** (Scheme 2)**.** Therefore, the HRMS spectra further confirmed the proposed mechanism.

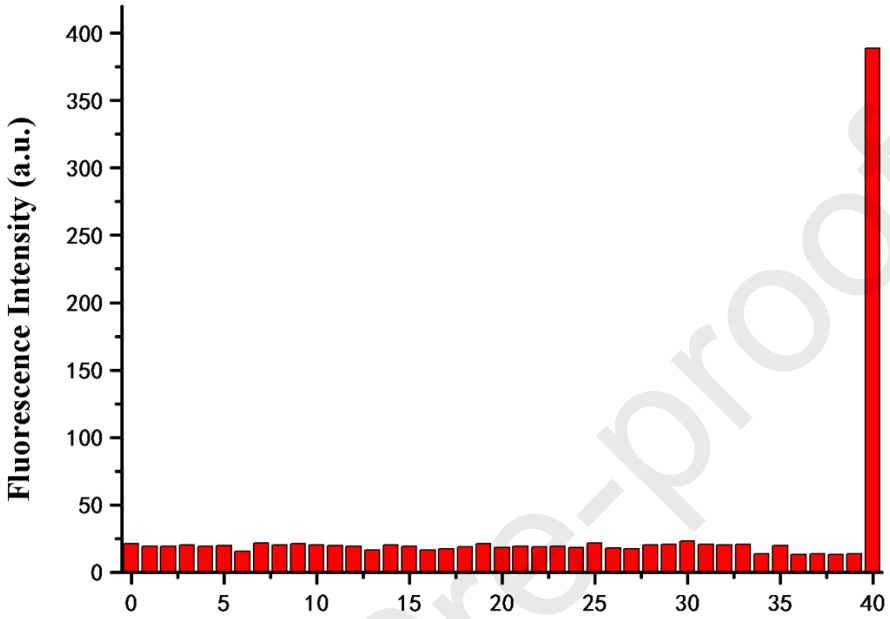

Figure 3 Fluorescence intensity at 637 nm of **FI-Mito** (1 μM) in the presence of various biological species in PBS buffer solution (pH = 8). 0: blank, 1: $AlCl_3$, 2: CH_3COONa, 3: KBr, 4: $CaCl_2$, 5: $CoCl_2$•$6H_2O$, 6: Na_2CO_3, 7: $CrCl_3$•$6H_2O$, 8: $CuCl_2$, 9: KF, 10: $NaHCO_3$, 11: $HgCl_2$, 12: Na_2HPO_4, 13: NaHS, 14: KI, 15: KCl, 16: LiF, 17: $MgCl_2$, 18: $MnCl_2$•$4H_2O$, 19: $NaNO_3$, 20: $Ni(NO_3)_2$•$6H_2O$, 21: $NaNO_2$, 22: KNO_3, 23: $PbCl_2$, 24: $Na_2S_2O_3$•$5H_2O$, 25: Na_2SO_4, 26: $SrCl_2$•$6H_2O$, 27: Alanine, 28: Asparagine, 29: Aspartic acid, 30: Glucose, 31: Homocysteine, 32: Nitric oxide, 33: Peroxynitrite, 34: Hydrogen peroxide, 35: Hydroxyl radical, 36: Singlet oxygen, 37: Superoxide radical anion, 38: TBHP, 39: *t*-BuO radical, 40: Sodium hypochlorite. Concentration: 50 μM for (1)-(26), 50 μM for (27)-(31), 10 μM for (32)-(39), and 1 μM for (40). λex = 580 nm.

To further gain some insight into **FI-Mito**'s selectivity, the fluorescence intensity (I_{637}) of **FI-Mito** was measured after addition of different biological species. As outlined in Fig. 3, when compared with ^{-}OCl, no apparent changes of I_{637} were

observed when other species were added. The tested relevant species (including ions, amino acids, ROS/RNS) even reaching up to high concentrations did not cause remarkable intensity increase. It could be concluded that **FI-Mito** exhibited desirable selectivity for $^{-}$OCl even in complex intracellular environment.

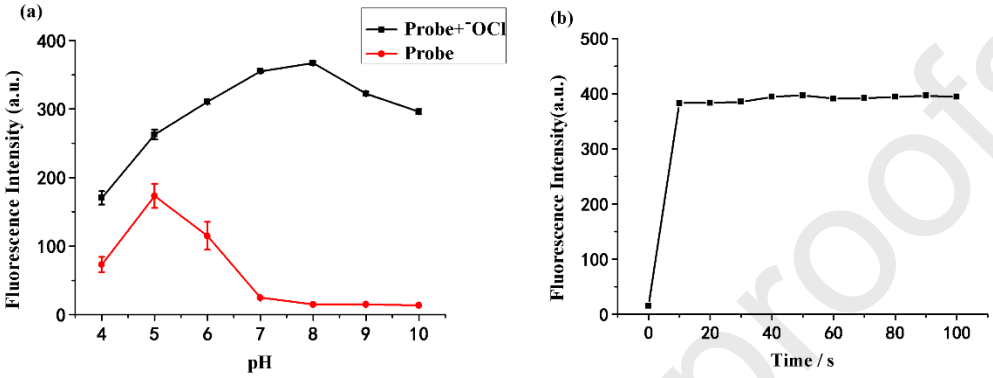

Figure 4 (a) Fluorescence intensity at 637 nm of **FI-Mito** versus pH in the absence (●) or presence (■) of $^{-}$OCl in 100% PBS buffer solution (pH 4-10). (b) Time-dependent fluorescence intensity at 637 nm of **FI-Mito** after addition of $^{-}$OCl in 100% PBS buffer solution (pH = 8). Conditions: [**FI-Mito**] = 1 μM, [$^{-}$OCl] = 1 μM, λex = 580 nm.

Subsequently, we inspected the pH effect on **FI-Mito**'s response to $^{-}$OCl (Fig. 4a). As a result, the probe alone did not emit fluorescence in alkaline pH conditions. The addition of $^{-}$OCl led to a significant enhancement of fluorescence intensity (I_{637}), especially in the weakly basic and neutral conditions. In view of the mitochondrial weakly basic pH [36], we believed that **FI-Mito** may provide a great platform well suited for the selective visualization of $^{-}$OCl in mitochondria.

The time course of **FI-Mito** was also evaluated since the response time was a critical indicator of a fluorescence probe. As shown in Fig. 4b, **FI-Mito** notably responded to $^{-}$OCl within 10 s and the fluorescence signal intensity almost remained constant up to 100 s. These results confirmed that probe **FI-Mito** was able to detect $^{-}$OCl rapidly with brilliant stability. Taken all together, the satisfying results from the in vitro experiments manifested that **FI-Mito** may act as a powerful tool for

hypochlorite detection in vivo.

*3.3 Cell imaging of probe **FI-Mito***

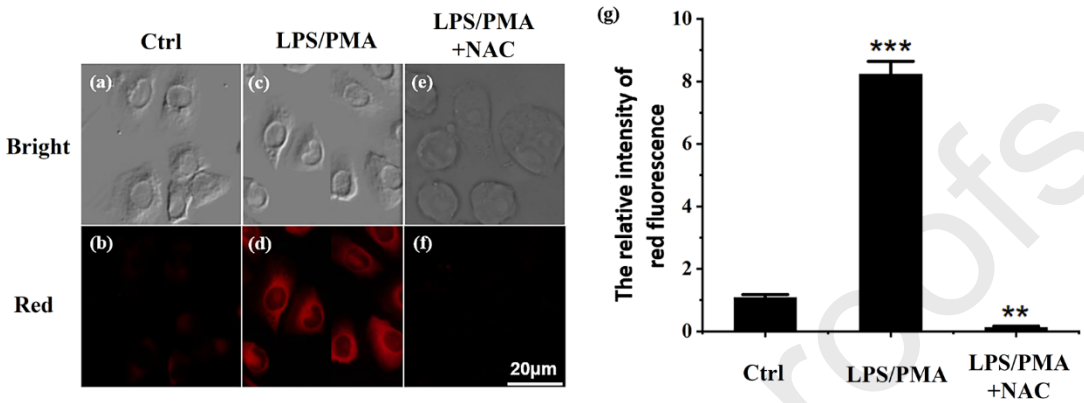

Figure 5 (a)-(f): Confocal fluorescence images of endogenously produced $^{-}$OCl in RAW264.7 cells with **FI-Mito**. First column (control): cells were treated only with **FI-Mito** (1 μM). Second column: cells were treated with incubation of LPS (1 μg/mL) for 6 h and PMA (1 μg/mL) for 30 min, and a subsequent incubation of **FI-Mito** (1 μM) for 30 min. Third column: cells pretreated with LPS (1 μg/mL) and PMA (1 μg/mL) were incubated with NAC (1 mM) for 1 h, and then with **FI-Mito** (1 μM) for 30 min. (g): Fluorescence intensity quantitation was analyzed by the Image J. The results were presented as mean ± SE with replicates n = 3. The fluorescence intensity from image (b) was defined as 1.0, ** $p < 0.01$, *** $p < 0.001$, as compared with the control. Statistical analyses were performed using the Student's *t*-test. Images were taken using an excitation laser of 561 nm and the corresponding fluorescence emissions were collected at 645-700 nm.

Since our probe **FI-Mito** displayed favorable optical characteristics for $^{-}$OCl detection in vitro (fast response, outstanding sensitivity and selectivity), experiments were carried out to estimate the ability to detect endogenous $^{-}$OCl in cells. In numerous studies it was proposed that the synergistic effect of lipopolysaccharide (LPS) and phorbol 12-myristate 13-acetate (PMA) could generate endogenous $^{-}$OCl in macrophages [37]. RAW264.7 cells were stimulated with 1 μg/mL LPS for 6 h, and

further incubated with 1 μg/mL PMA for 30 min, and then cells were incubated with **FI-Mito** (1 μM) for 30 min. After being washed with PBS for three times, the cells were imaged by the Leica SP8 confocal laser scanning microscope with a 20 × 0.7 NA objective lens. As outlined in Fig. 5d, bright rhodamine fluorescence was obviously noticed. By contrast, in the control group, cells were only incubated with **FI-Mito** in the absence of LPS and PMA. The red fluorescence of rhodamine was quite weak (Fig. 5b). Moreover, we performed an experiment using N-acetylcysteine (NAC), which was a commonly used scavenger of $^{-}$OCl [13]. The cells were pre-incubated in a sequence with LPS, PMA and further incubated with NAC (1 mM) for 1 h, then cells were incubated with **FI-Mito** for 30 min. Fig. 5f indicated that the fluorescence enhancement could be largely inhibited by NAC. The phenomena suggested that **FI-Mito** specifically reacted with $^{-}$OCl in RAW264.7 cells. The probe was capable of detecting endogenously induced $^{-}$OCl in macrophages.

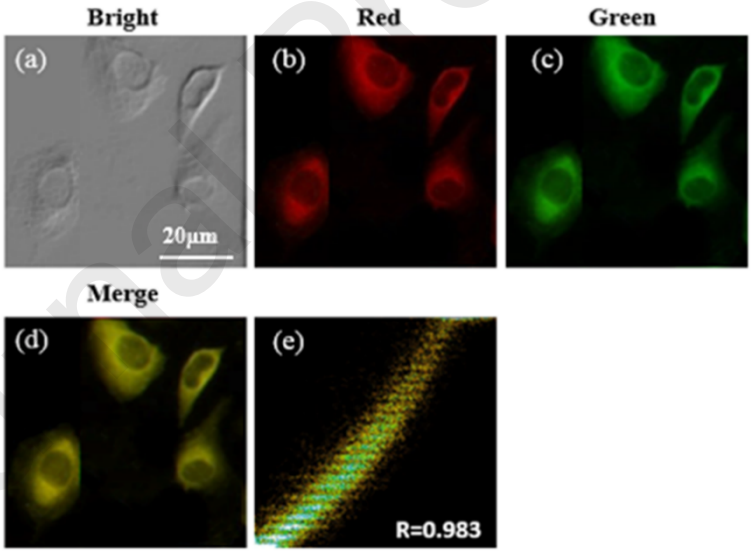

Figure 6 Fluorescence images of RAW264.7 cells co-stained with **FI-Mito** and Mito Tracker Deep Red. RAW264.7 cells were pretreated with LPS (1 μg/mL) for 6 h and then with PMA (1 μg/mL) for 30 min, followed by incubation with **FI-Mito** (1 μM) for 30 min. Then, the cells were incubated with Mito Tracker Deep Red (0.2 μM) for 30 min. (a) Bright field image. (b) Fluorescence of **FI-Mito** (red). (c) Fluorescence of Mito Tracker Deep Red (green). (d) Merge image of (b) and (c). (e) The intensity

scatter plot of red and green channels. Co-localization coefficient: 0.983. Imaging experiments were conducted on a Leica SP8 confocal laser scanning microscope with excitations at either 561 nm (for **FI-Mito**) and 638 nm (for Mito Tracker Deep Red) through a 20 × 0.7 NA objective; the corresponding fluorescence emissions were collected at 645-700 nm (for **FI-Mito**), 650-720 nm (for Mito Tracker Deep Red), respectively.

As previously reported in the literature, quaternized pyridine was a mitochondria-targeting moiety, which could increase the distribution of probe in mitochondria [18]. Inspired by this, we next performed the colocalization experiments to evaluate the subcellular distribution of **FI-Mito** by utilizing Mito Tracker Deep Red, a commercially available mitochondrial tracker (Fig. 6). Mito Tracker Deep Red was purchased from Invitrogen Corporation. Firstly, RAW264.7 cells pretreated with LPS (1 μg/mL) for 6 h and PMA (1 μg/mL) for 30 min were incubated with probe **FI-Mito** for 30 min. Then, the cells were incubated with Mito Tracker Deep Red (0.2 μM) for 30 min. Fig. 6 revealed that the emission of **FI-Mito** (Fig. 6b) fitted well with that of Mito Tracker Deep Red (Fig. 6c) and the merged images appeared yellow (Fig. 6d). Additionally, the intensity scatter plot of the red channel and green channel indicated a close correlation of the two emissions (Fig. 6e). The co-localization coefficient was 0.983, highlighting the superior efficacy of **FI-Mito** in targeting mitochondria.

Considering the molecular probe's cytotoxicity was an important parameter for bioanalytical applications, SRB assay was then performed by using probe **FI-Mito**. Fig. S5 (ESI†) implied that about 95% of RAW264.7 cells still remained alive after internalization of probe **FI-Mito** for 12 h. The data verified the excellent biocompatibility of **FI-Mito**.

3.4 Fluorescence imaging of $^{-}$OCl in living mice

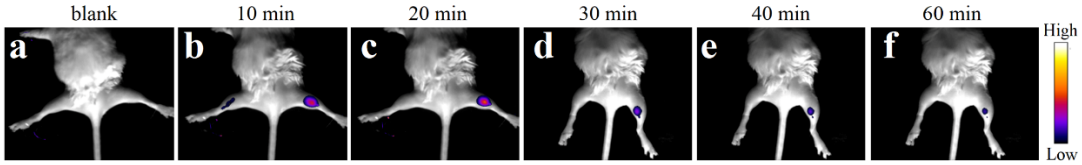

Figure 7 Representative fluorescence images of endogenous $^{-}$OCl in Kunming mice. (a) No treatment of **FI-Mito**. (b-f) LPS (5 μg/mL, 50 μL) and saline (50 μL) was injected into the right and left leg, respectively. 12 h later, 50 μL of **FI-Mito** (50 μM in saline, containing 1% DMSO) was injected into the same area in both of the legs. Images were recorded at different times: (b) 10 min; (c) 20 min; (d) 30 min; (e) 40 min; (f) 60 min. Images were taken using an excitation laser at 635 nm and a 676±30 nm bandpass filter.

Having studied the applicability of probe **FI-Mito** to detect $^{-}$OCl in living cells, we next tested its ability to image endogenously induced $^{-}$OCl in Kunming mouse. Firstly, the right leg of the mouse was given a skin-pop injection of LPS (5 μg/mL, 50 μL). The left leg was given a skin-pop injection of saline (50 μL) as control. After 12 hours, 50 μL of **FI-Mito** (50 μM in saline, containing 1% DMSO) was injected into the same region in both of the legs. And the images were obtained at different time points (Fig. 7). The bright fluorescence of the LPS-stimulated right leg was obviously noticed and the strongest signal was detected at 20 min. However, we hardly observed fluorescence in the left leg, which did not undergo the pre-treatment of LPS. The results indicated that **FI-Mito** may be used for the imaging of endogenous $^{-}$OCl in living mice.

Conclusion

In summary, we developed a selective and sensitive molecular probe for hypochlorite. The probe responded to hypochlorite with linearity and the detection limit was low (0.9 nM). Moreover, the probe was predominantly located in

mitochondria owing to the existence of the quaternized pyridine. Also, we applied it to visualize mitochondrial hypochlorite in both RAW264.7 cells and mice with minimal cytotoxicity. The data showed that the probe may serve as a practical indicator for hypochlorite in mitochondria with great biological significance.

Acknowledgement

The study was supported by the National Natural Science Foundation of China (21807078), Natural Science Foundation of Shandong Province (ZR2016BB35, ZR2018LB014) and Academic Promotion Programme of Shandong First Medical University (2019QL008).

Conflicts of interest

There are no conflicts to declare.

References

[1] H. Zhu, J.L. Fan, J.Y. Wang, H.Y. Mu, X.J. Peng, An “enhanced PET”-based fluorescent probe with ultrasensitivity for imaging basal and elesclomol-induced HClO in cancer cells, J. Am. Chem. Soc. 136 (2014) 12820-12823.

[2] Y.J. Gong, M.K. Lv, M.L. Zhang, Z.Z. Kong, G.J. Mao, A novel two-photon fluorescent probe with long-wavelength emission for monitoring HClO in living cells and tissues, Talanta 192 (2019) 128-134.

[3] J. Shepherd, S.A. Hilderbrand, P. Waternan, J.W. Heinecke, R. Weissleder, P. Libby, A fluorescent probe for the detection of myeloperoxidase activity in atherosclerosis-associated macrophages, Chem. Biol. 14 (2007) 1221-1231.

[4] C. Duan, M. Won, P. Verwilst, J.C. Xu, H.S. Kim, L.T. Zeng, J.S. Kim, In vivo imaging of endogenously produced HClO in zebrafish and mice using a bright, photostable ratiometric fluorescent probe, Anal. Chem. 91 (2019) 4172-4178.

[5] P. Wei, L.Y. Liu, Y. Wen, G.L. Zhao, F.F. Xue, W. Yuan, R.H. Li, Y.P. Zhong, M.F. Zhang, T. Yi, Release of amino- or carboxy-containing compounds triggered by

Journal Pre-proofs

HOCl: application for imaging and drug design, Angew. Chem. Int. Ed. 58 (2019) 4547-4551.

[6] Y. Huang, N. He, Y.D. Wang, L.W. Zhang, Q. Kang, Y.Q. Wang, D.Z. Shen, J. Choo, L.X. Chen, Detection of hypochlorous acid fluctuation via a selective near-infrared fluorescent probe in living cells and in vivo under hypoxic stress, J. Mater. Chem. B 7 (2019) 2557-2564.

[7] Y.R. Zhang, Y. Liu, X. Feng, B.X. Zhao, Recent progress in the development of fluorescent probes for the detection of hypochlorous acid, Sens. Actuators B 240 (2017) 18-36.

[8] H. Feng, Y. Wang, J.P. Liu, Z.Q. Zhang, X.Y. Yang, R. Chen, Q.T. Meng, R. Zhang, A highly specific fluorescent probe for rapid detection of hypochlorous acid in vivo and in water samples, J. Mater. Chem. B 7 (2019) 3909-3916.

[9] X.H. Li, X.H. Gao, W. Shi, H.M. Ma, Design strategies for water-soluble small molecular chromogenic and fluorogenic probes, Chem. Rev. 114 (2014) 590-659.

[10] X.Q. Chen, F. Wang, J.Y. Hyun, T.W. Wei, J. Qiang, X.T. Ren, I. Shin, J. Yoon, Recent progress in the development of fluorescent, luminescent and colorimetric probes for detection of reactive oxygen and nitrogen species, Chem. Soc. Rev. 45 (2016) 2976-3016.

[11] R.G. Shi, H. Chen, Y.P. Qi, W. Huang, G. Yin, R.Y. Wang, From aggregation-induced to solution emission: a new strategy for designing ratiometric fluorescent probes and its application for in vivo HClO detection, Analyst 144 (2019) 1696-1703.

[12] D.L. Shi, S.Q. Chen, B. Dong, Y.H. Zhang, C.Q. Sheng, T.D. James, Y. Guo, Evaluation of HOCl-generating anticancer agents by an ultrasensitive dual-mode fluorescent probe, Chem. Sci. 10 (2019) 3715-3722.

[13] J. Zhou, L.H. Li, W. Shi, X.H. Gao, X.H. Li, H.M. Ma, HOCl can appear in the mitochondria of macrophages during bacterial infection as revealed by a sensitive mitochondrial-targeting fluorescent probe, Chem. Sci. 6 (2015) 4884-4888.

[14] Y.J. Zuo, Y. Zhang, B.L. Dong, Z.M. Gou, T.X. Yang, W.Y. Lin, Binding reaction sites to polysiloxanes: unique fluorescent probe for reversible detection of

Journal Pre-proofs

ClO^-/GSH pair and the in situ imaging in live cells and zebrafish, Anal. Chem. 91 (2019) 1719-1723.

[15] T. Kuhana A, W.Y. Feng, G.Q. Feng, A simple but effective colorimetric and far-red to near-infrared fluorescent probe for palladium and its application in living cells, Dyes Pigm. 152 (2018) 112-117.

[16] F.L. Zhang, Y.Z. Di, Y. Li, Q.K. Qi, J.Y. Qian, X.Q. Fu, B. Xu, W.J. Tian, Highly efficient far Red/near-Infrared fluorophores with aggregation-induced emission for bioimaging, Dyes Pigm. 142 (2017) 491-498.

[17] F.S. Tian, Y. Jia, Y.N. Zhang, W. Song, G.J. Zhao, Z.J. Qu, C.Y. Li, Y.H. Chen, P. Li, A HClO-specific near-infrared fluorescent probe for determination of myeloperoxidase activity and imaging mitochondrial HClO in living cells, Biosens. Bioelectron. 86 (2016) 68-74.

[18] S.L. Shen, X. Zhao, X.F. Zhang, X.L. Liu, H. Wang, Y.Y. Dai, J.Y. Miao, B.X. Zhao, A mitochondria-targeted ratiometric fluorescent probe for hypochlorite and its applications in bioimaging, J. Mater. Chem. B 5 (2017) 289-295.

[19] S.L. Shen, X.F. Zhang, Y.Q. Ge, Y. Zhu, X.Q. Cao, A mitochondria-targeting ratiometric fluorescent probe for the detection of hypochlorite based on the FRET strategy, RSC Adv. 7 (2017) 55296-55300.

[20] L. Yuan, L. Wang, B.K. Agrawalla, S.J. Park, H. Zhu, B. Sivaraman, J.J. Peng, Q.H. Xu, Y.T. Chang, Development of targetable two-photon fluorescent probes to image hypochlorous acid in mitochondria and lysosome in live cell and inflamed mouse model, J. Am. Chem. Soc. 137 (2015) 5930-5938.

[21] K. Li, J.T. Hou, J. Yang, X.Q. Yu, A tumor-specific and mitochondria-targeted fluorescent probe for real-time sensing of hypochlorite in living cells, Chem. Commun. 53 (2017) 5539-5541.

[22] X.J. Jiao, K. Huang, S. He, C. Liu, L.C. Zhao, X.S. Zeng, A mitochondria-targeted near-infrared fluorescent probe with a large Stokes shift for real-time detection of hypochlorous acid, Org. Biomol. Chem. 17 (2019) 108-114.

[23] S.L. Shen, X.Q. Huang, H.L. Jiang, X.H. Lin, X.Q. Cao, A rhodamine B-based probe for the detection of HOCl in lysosomes, Anal. Chim. Acta 1046 (2019)

Journal Pre-proofs

185-191.

[24] S.L. Shen, X.Q. Huang, X.H. Lin, X.Q. Cao, A ratiometric fluorescent probe for lysosomal hypochlorous acid based on through-bond energy transfer strategy, Anal. Chim. Acta 1052 (2019) 124-130.

[25] S.L. Shen, X.Q. Huang, Y.Y. Zhang, Y. Zhu, C. Hou, Y.Q. Ge, X.Q. Cao, Ratiometric fluorescent probe for the detection of HOCl in lysosomes based on FRET strategy, Sens. Actuators B 263 (2018) 252-257.

[26] M.G. Ren, B.B. Deng, K. Zhou, X.Q. Kong, J.Y. Wang, G.P. Xu, W.Y. Lin, A lysosome-targeted and ratiometric fluorescent probe for imaging exogenous and endogenous hypochlorous acid in living cells, J. Mater. Chem. B 4 (2016) 4739-4745.

[27] Y.F. Huang, Y.B. Zhang, F.J. Huo, J.B. Chao, C.X. Yin, A near-infrared ratiometric fluorescent probe with large stokes based on isophorone for rapid detection of ClO^- and its bioimaging in cell and mice, Sens. Actuators B 287 (2019) 453-458.

[28] J.T. Hou, M.Y. Wu, K. Li, J. Yang, K.K. Yu, Y.M. Xie, X.Q. Yu, Mitochondria-targeted colorimetric and fluorescent probes for hypochlorite and their applications for in vivo imaging, Chem. Commun. 50 (2014) 8640-8643.

[29] P. Wei, W. Yuan, F.F. Xue, W. Zhou, R.H. Li, D.T. Zhang, T. Yi, Deformylation reaction-based probe for in vivo imaging of HOCl, Chem. Sci. 9 (2018) 495-501.

[30] D. Wu, J.C. Ryu, Y.W. Chung, D. Lee, J.H. Ryu, J.H. Yoon, J. Yoon, A far-red-emitting fluorescence probe for sensitive and selective detection of peroxynitrite in live cells and tissues, Anal. Chem. 89 (2017) 10924-10931.

[31] G.J. Mao, G.Q. Gao, Z.Z. Liang, Y.Y. Wang, L. Su, Z.X. Wang, H. Zhang, Q.J. Ma, G.S. Zhang, A mitochondria-targetable two-photon fluorescent probe with a far-red to near-infrared emission for sensing hypochlorite in biosystems, Anal. Chim. Acta 1081 (2019) 184-192.

[32] Y.Q. Sun, J. Liu, X. Lv, Y.L. Liu, Y. Zhao, W. Guo, Rhodamine-inspired far-red to near-infrared dyes and their application as fluorescence probes, Angew. Chem. Int. Ed. 51 (2012) 7634-7636.

Journal Pre-proofs

[33] H. Meng, X.Q. Huang, Y. Lin, D.Y. Yang, Y.J. Lv, X.Q. Cao, G.X. Zhang, J. Dong, S.L. Shen, A new ratiometric fluorescent probe for sensing lysosomal HOCl based on fluorescence resonance energy transfer strategy, Spectrochim. Acta A Mol. Biomol. Spectrosc. 223 (2019), 117355.

[34] M.G. Ren, Z.H. Li, B.B. Deng, L. Wang, W.Y. Lin, Single fluorescent probe separately and continuously visualize H_2S and HClO in lysosomes with different fluorescence signals, Anal. Chem. 91 (2019) 2932-2938.

[35] L. Yuan, W.Y. Lin, Y.N. Xie, B. Chen, J.Z. Song, Fluorescent detection of hypochlorous acid from turn-on to FRET-based ratiometry by a HOCl-mediated cyclization reaction, Chem. Eur. J. 18 (2012) 2700-2706.

[36] J.T. Hou, K. Li, J. Yang, K.K. Yu, Y.X. Liao, Y.Z. Ran, Y.H. Liu, X.D. Zhou, X.Q. Yu, A ratiometric fluorescent probe for in situ quantification of basal mitochondrial hypochlorite in cancer cells, Chem. Commun. 51 (2015) 6781-6784.

[37] L. Yuan, W.Y. Lin, H. Chen, Analogs of Changsha near-infrared dyes with large Stokes Shifts for bioimaging, Biomaterials 34 (2013) 9566-9571.

[38] J. Kang, F.J. Huo, Y.B. Zhang, J.B. Chao, R.M. Strongin, C.X. Yin, Detecting intracellular ClO^- with ratiometric fluorescent signal and its application in vivo, Sens. Actuators B 273 (2018) 1532-1538.

Journal Pre-proofs

Tian-Ran Wang: Methodology, Data curation, Software.

Xiao-Fan Zhang: Writing-Original draft preparation, Writing-Reviewing and Editing.

Xiao-Qing Huang: Data curation, Methodology.

Xiao-Qun Cao: Visualization, Investigation.

Shi-Li Shen: Conceptualization, Supervision, Software, Validation.

Journal Pre-proofs

Declaration of interests

☒ The authors declare that they have no known competing financial interests or personal relationships that could have appeared to influence the work reported in this paper.

☐The authors declare the following financial interests/personal relationships which may be considered as potential competing interests:

Journal Pre-proofs

Graphical abstract

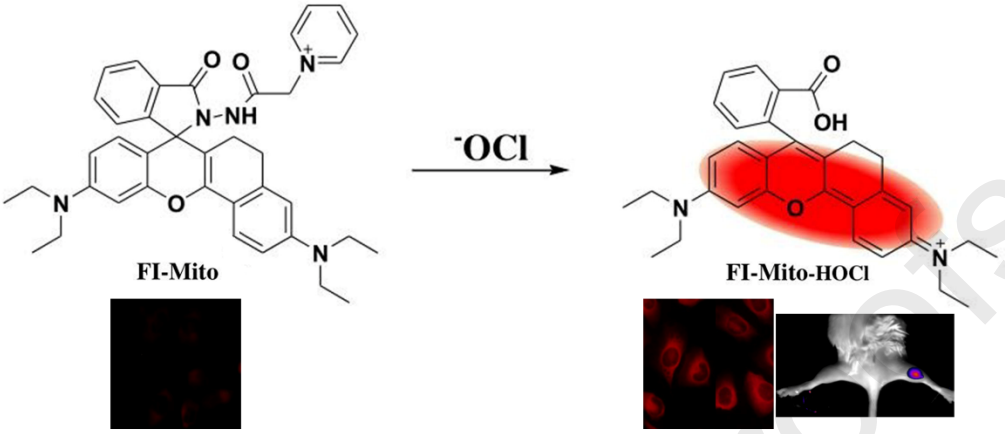

A mitochondria-targeting fluorescent probe (**FI-Mito**) for $^{-}$OCl was developed based on rhodamine dye. More importantly, **FI-Mito** was capable of detecting endogenous $^{-}$OCl both in RAW264.7 cells and living mouse.

Journal Pre-proofs

Highlights

- A novel fluorescent probe for $^{-}$OCl was developed based on rhodamine dye.
- The probe could monitor $^{-}$OCl changes with outstanding sensitivity, selectivity and rapid response in the far-red to near-infrared region.
- The probe could target mitochondria with little cytotoxicity.
- The probe was successfully applied to image endogenous $^{-}$OCl in RAW264.7 cells and living mice.

Journal Pre-proofs